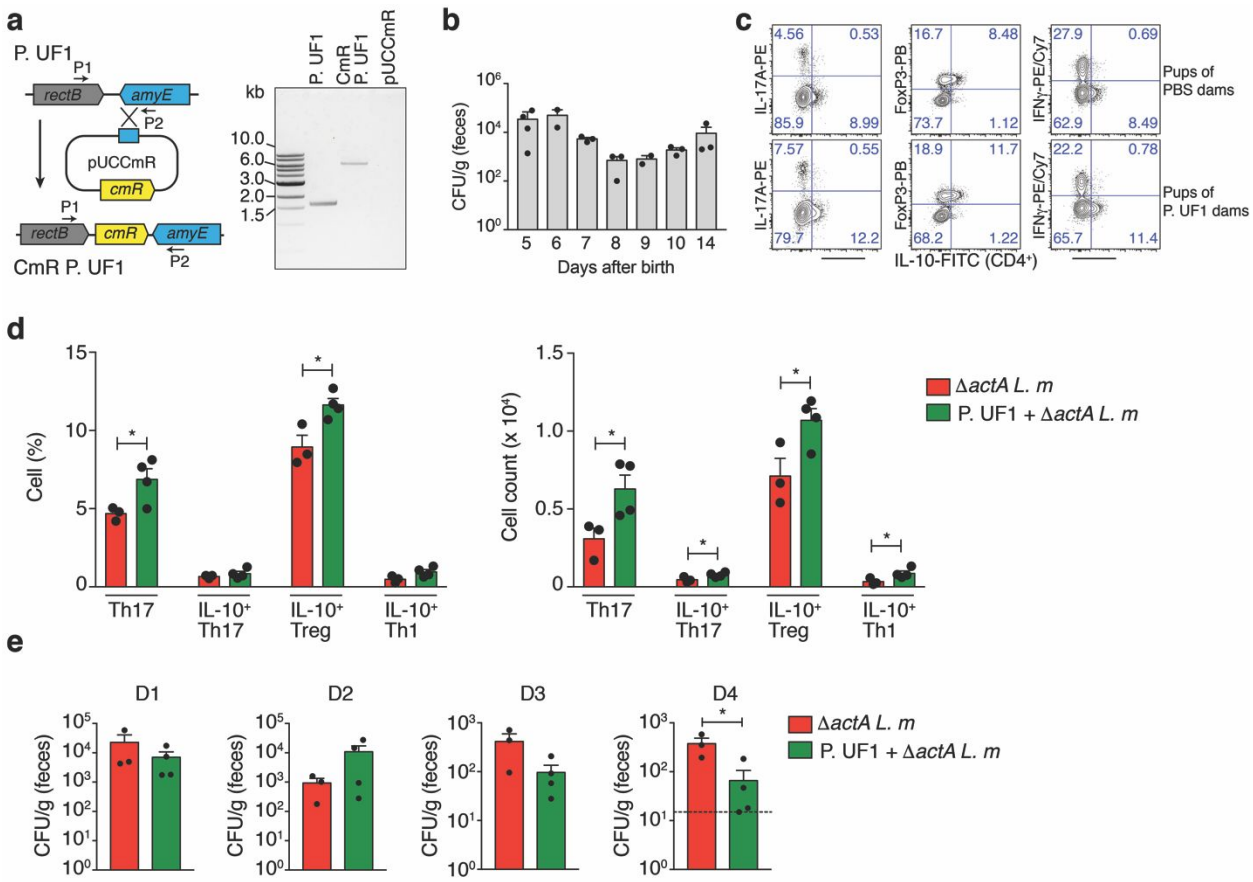

Supplementary Fig. 1 Maternal effects mediated by P. UF1. **a** Genetic construction of antibiotic-resistant P. UF1 strain. The chloramphenicol resistant gene (*CmR*) was inserted into the non-essential region downstream of alpha-amylase gene (*amyE*) by homologous recombination, resulting in CmR P. UF1 strain. PCR identification of chromosomal insertion using primers P1 and P2 is shown. **b** C57BL/6 dams were gavaged with CmR P. UF1 (10^9 CFU/dam, twice a week) during pregnancy. After birth, newborn mice were kept with their mothers that were gavaged with CmR P. UF1. Newborn mice (n = 2-3) were sacrificed at days 5-14 to collect luminal contents. The CmR P. UF1-transfer into the newborn mice was determined by plating the fecal contents on the chloramphenicol-resistant MRS-lactate agar plates. **c-e** C57BL/6 dams were gavaged with P. UF1 (10^9 CFU/dam, twice a week), or PBS during pregnancy. After birth, newborn mice were not gavaged with P. UF1, or PBS and kept 21 days with their mothers that were gavaged with P. UF1 (10^9 CFU/dam, twice a week), or PBS. Newborn mice (n = 3-4) were then orally infected with Δ*actA L. m* (10^8 CFU/mouse) and

euthanized 7 days post infection to analyze colonic $CD4^+$ T cell response. (**c**) Representative flow plots for colonic IL-10^+ Th17, IL-10^+ $FoxP3^+$ Tregs and IL-10^+ IFNγ^+ Th1 cells. (**d**) Frequency and total counts of colonic Th17, IL-10^+ Th17, IL-10^+ $FoxP3^+$ Tregs and IL-10^+ IFNγ^+ Th1 cells from newborn mice delivered by P. UF1- or PBS-gavaged dams. (**e**) Bacterial burdens of Δ*actA L. m* in feces of new mice. Dash line indicates the limit of detection. Data are from 1 experiment (**c**-**e**), or pooled from 3 experiments (**b**). Data are presented as mean ± SEM; * $p < 0.05$, 2-tailed unpaired *t*-test.

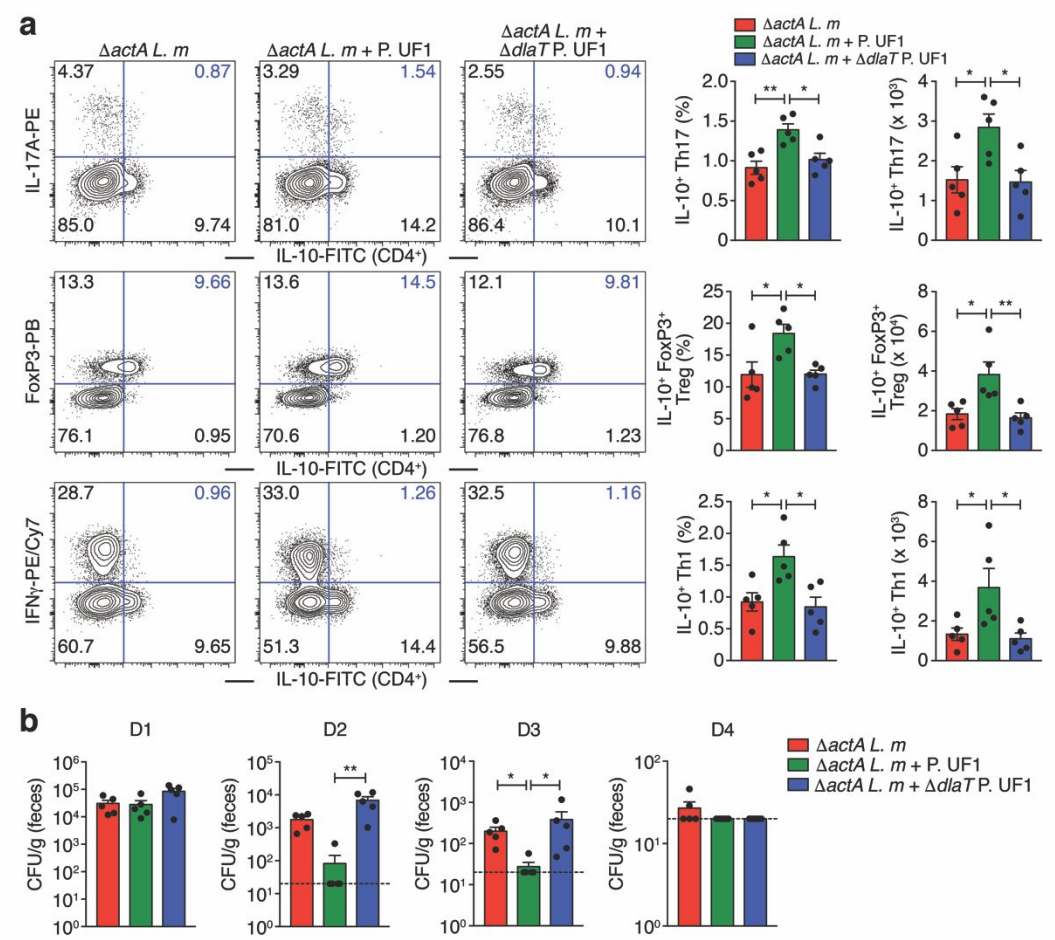

Supplementary Fig. 2 T helper cells induced by P. UF1 protect neonatal mice against *L. m* infection. Pregnant C57BL/6 dams were gavaged weekly with P. UF1, Δ*dlaT* P. UF1 (10^9 CFU/dam) or PBS. After birth, newborn mice of the respective dams were gavaged weekly with P. UF1, Δ*dlaT* P. UF1 (10^7 CFU/mouse), or PBS during breastfeeding. After weaning, mice continued to receive one gavage of P. UF1, Δ*dlaT* P. UF1 (10^8 CFU/mouse), or PBS. One day after the last gavage, mice (n = 5) were infected with Δ*actA L. m* (10^9 CFU/mouse) and euthanized 7 days post infection to analyze colonic $CD4^+$ T cell responses. **a** Representative flow plots, frequency and total cell counts of IL-10^+ Th17, IL-10^+ $FoxP3^+$ Treg and IL-10^+ $IFN\gamma^+$ Th1 cells. **b** Bacterial burdens of Δ*actA L. m* in feces of mice from the indicated groups. Dash lines indicate the limit of detection. Data are from 1 experiment and presented as mean ± SEM; * $p < 0.05$, ANOVA plus Tukey post-test (**a**) or Kruskal-Wallis test (**b**).

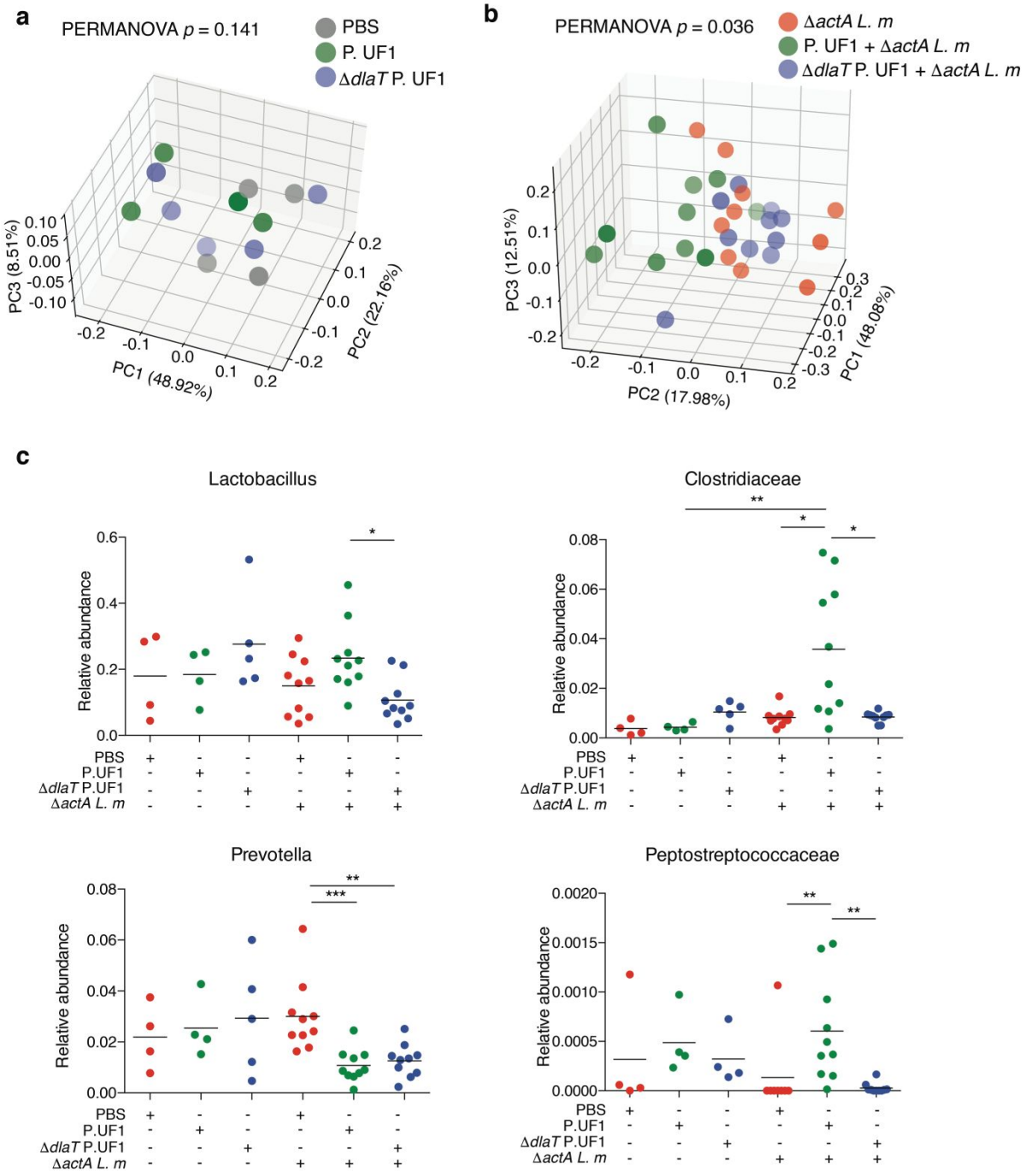

Supplementary Fig. 3 P. UF1 modulates the microbiota composition during Δ*actA L. m* infection. **a** Pregnant C57BL/6 dams were gavaged weekly with P. UF1, Δ*dlaT* P. UF1 (10^9 CFU/dam), or PBS. After birth, newborn mice (n = 4-5) of the respective dams continued to receive PBS, P. UF1, or Δ*dlaT* P. UF1 (10^7 CFU/mouse during breastfeeding, 10^8 CFU/mouse

after weaning, once a week) until 8 weeks of age. Fecal samples were collected for microbiota analysis before Δ*actA L. m* infection. Principal coordinate analysis (PcoA) plot showing that the fecal microbiomes of the indicated groups were not significantly separated (PERMANOVA test, $p = 0.141$). **b** 8-week-old mice (n = 10) receiving the same treatment were orally infected with Δ*actA L. m*. 7 days post infection, fecal samples were collected for microbiota analysis. Significant separation of microbial communities derived from mouse groups after Δ*actA L. m* infection (PERMANOVA test, $p = 0.036$). **c** Relative abundances of selected taxa in the indicated groups before and after Δ*actA L. m* infection. Data are from 1 (**a**), or 2 (**b**) experiments; Data are presented as mean; * $p < 0.05$, ** $p < 0.01$, *** $p < 0.001$, Kruskal-Wallis test plus Dunn's multiple comparisons test (**c**).

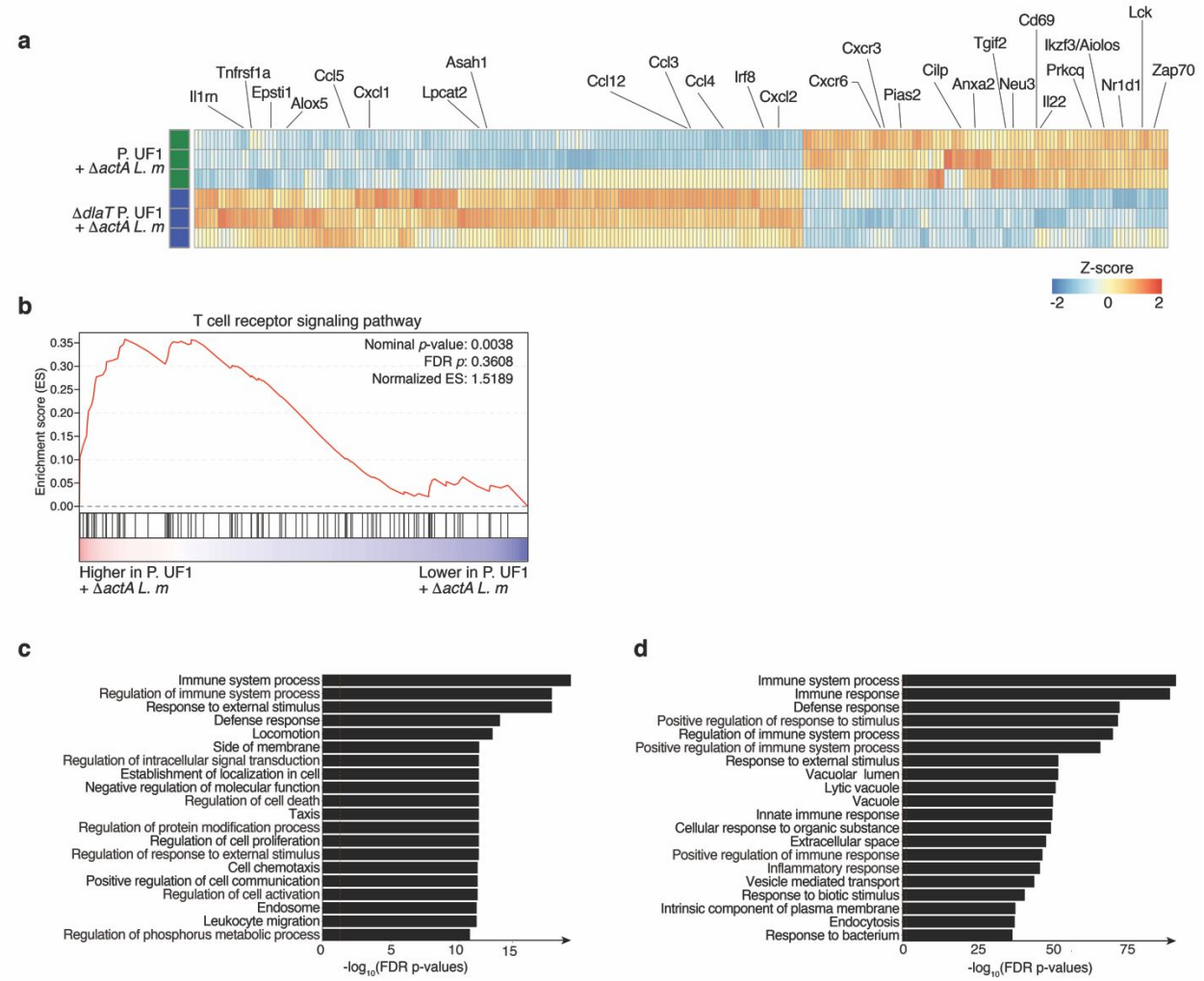

Supplementary Fig. 4 DlaT-dependent regulation of Th17 cells during Δ*actA L. m* infection. **a** Heatmap of z-scores of regularized-log-transformed normalized counts of genes from sorted Th17 cells isolated from IL-17A^{eGFP} mice (filtered by FDR $p < 0.05$). **b** Representative GSEA plot for T cell receptor signaling pathway from KEGG database. **c** Enriched gene sets elevated in Th17 cells derived from P. UF1-gavaged mice compared to Th17 cells isolated from Δ*dlaT* P. UF1-gavaged mice. **d** Enriched gene sets downregulated in P. UF1-induced Th17 cells compared to Th17 cells derived from Δ*dlaT* P. UF1-gavaged mice.

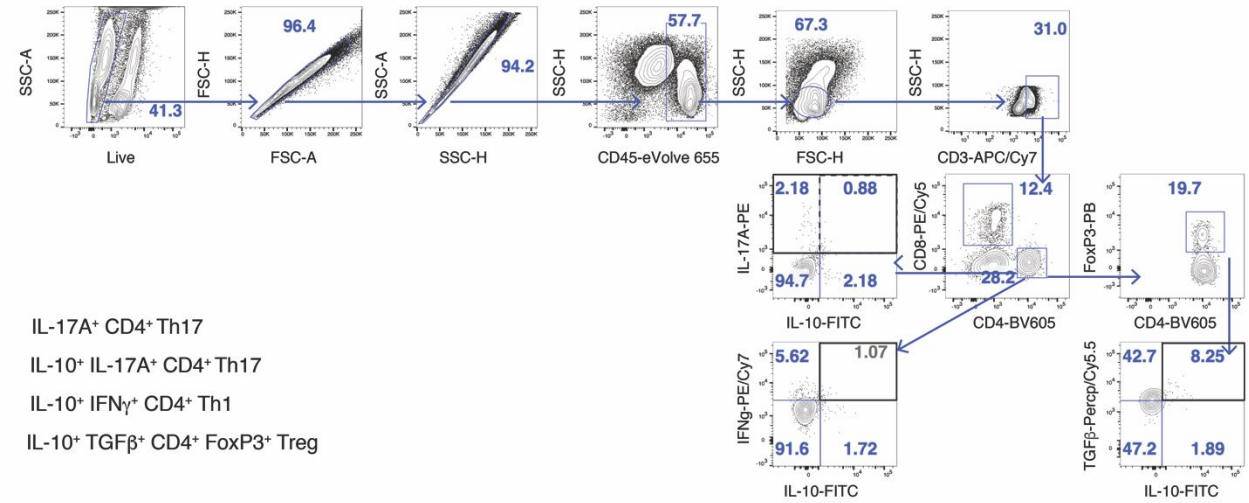

Supplementary Fig. 5 Flow cytometric gating strategy for Th17, IL-10$^+$ Th17, IL-10$^+$ TGFβ^+ Treg and IL-10$^+$ IFNγ^+ Th1 cells. Colonic cells were isolated, stimulated with PMA/ionomycin, and analyzed using flow cytometry. After dead and doublet cell exclusion, CD45$^+$ cells were selected. Lymphocytes were gated on FSC-H versus SSC-H followed by CD3$^+$ and subsequently on CD4$^+$ CD8$^-$ events. The cytokine-positive (IL-10$^+$, IL-17A$^+$, IFNγ^+, TGFβ^+) cells in CD4$^+$ CD8$^-$ compartment were then evaluated.